J Membrane Biol (2011) 239:15–26
DOI 10.1007/s00232-010-9324-8

# Determining Peptide Partitioning Properties via Computer Simulation

**Jakob P. Ulmschneider · Magnus Andersson · Martin B. Ulmschneider**

Received: 15 September 2010 / Accepted: 5 November 2010 / Published online: 25 November 2010


**Abstract** The transfer of polypeptide segments into lipid bilayers to form transmembrane helices represents the crucial first step in cellular membrane protein folding and assembly. This process is driven by complex and poorly understood atomic interactions of peptides with the lipid bilayer environment. The lack of suitable experimental techniques that can resolve these processes both at atomic resolution and nanosecond timescales has spurred the development of computational techniques. In this review, we summarize the significant progress achieved in the last few years in elucidating the partitioning of peptides into lipid bilayer membranes using atomic detail molecular dynamics simulations. Indeed, partitioning simulations can now provide a wealth of structural and dynamic information. Furthermore, we show that peptide-induced bilayer distortions, insertion pathways, transfer free energies, and kinetic insertion barriers are now accurate enough to complement experiments. Further advances in simulation methods and force field parameter accuracy promise to turn molecular dynamics simulations into a powerful tool for investigating a wide range of membrane active peptide phenomena.

**Keywords** Biophysical techniques in membrane research · Membrane structure (protein and lipid diffusion) · Structure of membrane proteins · Peptide partitioning · Water to bilayer transfer of peptides

J. P. Ulmschneider
IWR, University of Heidelberg, Heidelberg, Germany
e-mail: jakob@ulmschneider.com

M. Andersson (✉) · M. B. Ulmschneider
Department of Physiology and Biophysics, University of California at Irvine, Irvine, CA, USA
e-mail: magnus.andersson@uci.edu

M. B. Ulmschneider
e-mail: martin@ulmschneider.com

## The Importance of Peptide Partitioning Studies

Membrane protein folding and assembly is thought to be a two-stage process in which transmembrane (TM) helices are first individually established in the bilayer and subsequently rearranged to form the functional protein (Jacobs and White 1989; Popot and Engelman 1990). However, because of the complex and highly dynamic interactions of peptides with the lipid bilayer environment, the mechanisms and energetics underlying this process are poorly understood. In this review, we summarize recent computational efforts to estimate the free energy of transfer of polypeptide segments into membranes. Precise partitioning energetics provide fundamental insights into the folding and assembly process of membrane proteins. Moreover, such knowledge will significantly improve existing computational methodologies (e.g., force fields) for ab initio structure prediction and simulation of membrane proteins.

Current experimental techniques lack the combination of spatial (atomic) and temporal (nanosecond) resolution needed for a direct observation of partitioning phenomena. Furthermore, designing experiments to measure equilibrium thermodynamic and kinetic transfer properties of peptides into lipid bilayers has proved difficult, primarily because sequences that are sufficiently hydrophobic to insert without disrupting the membrane have a tendency to aggregate (Ladokhin and White 2004; Wimley and White 2000). To avoid these difficulties, the cellular translocon machinery has recently been utilized to insert polypeptide segments with systematically designed sequences into the endoplasmic reticulum membrane, thereby providing the

first experimental estimate of the insertion energetics of arbitrary peptides (Hessa et al. 2005a, 2007). Interestingly, the results correlate strongly with experimental whole residue water-to-octanol transfer free energy scales (Wimley et al. 1996). However, the biological scale might reflect the partitioning of peptides between the translocon channel and the bilayer, rather than water and bilayer. In the absence of direct water-to-bilayer partitioning data, this issue cannot at present be unambiguously resolved.

Recently, extended molecular dynamics (MD) simulations have been able to reach the temporal realm in which the partitioning of monomeric hydrophobic peptides into lipid bilayers takes place. It has therefore become possible to study the partitioning phenomena quantitatively at atomic-level resolution. Here we summarize recent progress and key results in simulation studies of the partitioning process.

## Simplified Membrane Models

The key difficulty in folding–partitioning simulations is sampling. Spontaneous partitioning of peptides into membranes generally requires micro- to milliseconds of simulation. Early computational attempts therefore utilized simplified mean-field models, where the water and membrane were represented implicitly as a continuum, the so-called implicit membrane methods (for a recent review of these models, see Ulmschneider and Ulmschneider 2010). This greatly speeds up peptide sampling by reducing the computer time spent on the solvent. The most advanced implicit membrane methods are based on the generalized Born theory for ionic solvation, and their application to small hydrophobic peptides has provided a confirmation of the theoretically predicted folded insertion pathway and rough estimates of the energetics involved (Im and Brooks 2005; Ulmschneider and Ulmschneider 2007, 2008b). However, these models cannot account for many important bilayer effects such as hydrogen bonding and hydration of the lipid head group environment and bilayer distortions due to, e.g., hydrophobic mismatch, as the membrane is reduced to essentially a low dielectric continuum.

A similar but conceptually different approach is the use of coarse-grained (CG) models (Lindahl and Sansom 2008). Here adjacent atoms are fused together into "beads" to reduce the total number of nonbonded interactions that have to be computed. Numerous applications to long-timescale peptide–membrane phenomena have been reported, such as the aggregation and poroidal insertion of antimicrobial and cell-penetrating peptides, and the formation of TM helix bundles from individually inserted helices (see Gurtovenko et al. 2010 for an extensive recent review). Despite these successes, the ability of CG to quantitatively reproduce partitioning phenomena appears restricted. Typical drawbacks are the lack of hydrogen bonds and the absence of water polarizability, as well as CG water beads that are too big to pass through membrane pores or act as buried structural water. The most severe limitation of CG methods is their inherent requirement to fix the protein secondary and tertiary structure through use of restraints or scaffolding interactions. This greatly reduces the predictive power and credibility of these simulations.

To extract quantitative partitioning data from peptide–membrane simulations, it is preferable to use unbiased atomic detail methods that capture all physiochemical interactions accurately. For the rest of this review, we will therefore concentrate on atomistic simulations, which provide a more truthful representation of the peptide partitioning phenomena. Recent simulation results have demonstrated that the timescales required to observe complete peptide–membrane adsorption, folding, and insertion processes can now be reached (Ulmschneider et al. 2010a). For partitioning studies, there is therefore probably no further need to use less accurate and simplified methods.

## Potential of Mean Force Methods

Atomic detail membrane simulations are superior to all other methods in terms of accuracy, realism, and predictive power. They directly account for structural water molecules and accurate treatment of hydrogen bonds, capture the reordering of solvents via polarization, and reproduce entropic effects due to lipid tail order and bilayer deformations. However, all this comes at the cost of requiring significantly larger computational resources. Consequently, simulations have been kept rather short. Typical lengths are in the $t < 200$ ns range, too short to directly observe water-to-bilayer peptide partitioning (Freites et al. 2005).

Instead, the preferred approach has been to use umbrella sampling and related free energy methods to obtain the insertion energetics and potentials of mean force (PMF) along the membrane normal. These studies have ranged from PMFs for amino acid side chain analogues (Johansson and Lindahl 2008; MacCallum et al. 2008), individual amino acids on helical scaffold peptides (Li et al. 2008a), and a synthetic model hexapeptide (Babakhani et al. 2008). These PMF calculations have helped to improve our understanding of the preferred orientation and location of peptides in membranes as well as associated peptide-induced bilayer perturbations. In addition, PMFs have provided more accurate estimates of the transfer free energies of individual amino acids into the bilayer. We will describe in detail below how these methods have been used to study the energetics of arginine partitioning.

It is, however, difficult to predict full-peptide partitioning data of relevant sequences (e.g., antimicrobials) from insertion scales of side chain analogues (lacking backbone contributions) or individual amino acids because these potentials are not simply additive and strongly vary with sequence position, folding state, and adjacent residues that can either act cooperatively or not. PMFs should therefore ideally be obtained for full peptides. One drawback of PMF calculations is the potential lack of convergence due to incomplete sampling at critical parts along the constraint coordinate that can lead to incorrect free energy estimates and hysteresis effects. In addition, these simulations spend most of their sampling time in high-energy transition-barrier regions of phase space that are never really populated in equilibrium. A simple alternative is to study full-peptide partitioning using conventional equilibrium simulations. The success of this approach appears to hint that the current trend to approach biomolecular questions by use of restraining potentials, umbrella sampling, and pulling forces can lead scientists to overlook the fact that sometimes these processes can be much more easily studied by simple equilibrium simulations.

## Atomic Detail Partitioning Simulations: The Importance of Accurate Parameters

Studying water-to-bilayer partitioning phenomena directly with conventional MD simulations requires sufficient sampling. Previously, this was thought to be unfeasible as a result of the millisecond-level timescales necessary to ensure that the process is captured in its entirety. However, this has turned out to be an overestimation, with completely converged peptide partitioning studies requiring as little as 1–2 μs in some cases, depending on the kinetic insertion barrier of the peptide.

Crucial to the success of these simulations is the careful calibration and verification of force field parameters to ensure that the strength of the protein–lipid interactions is accurately reproduced. At the time of their design, most force fields could not be tested beyond the pico- to nanosecond range (Freddolino et al. 2008), making their extension to multimicrosecond simulations potentially problematic.

Indeed, the first nanosecond-timescale replica exchange partitioning simulation performed with an atomic lipid bilayer representation showed that a highly helical WALP peptide (sequence: ace-AWW-$(LA)_5$-WWA-ame) (Killian 2003) inserted into the lipid bilayer while fully extended (Nymeyer et al. 2005) (Fig. 1a). Subsequent multimicrosecond MD simulations (Ulmschneider and Ulmschneider 2008a) of the same peptide not only replicated the unfolded insertion pathway, but also found stable unfolded conformations as the energetically favored native state even though a different force field was used (Fig. 1b) (Ulmschneider and Ulmschneider 2008a, 2009a).

The results from these two pioneering partitioning studies are in direct contradiction to a vast body of experimental evidence and careful theoretical considerations (reviewed in White 2006; White and Wimley 1999), which

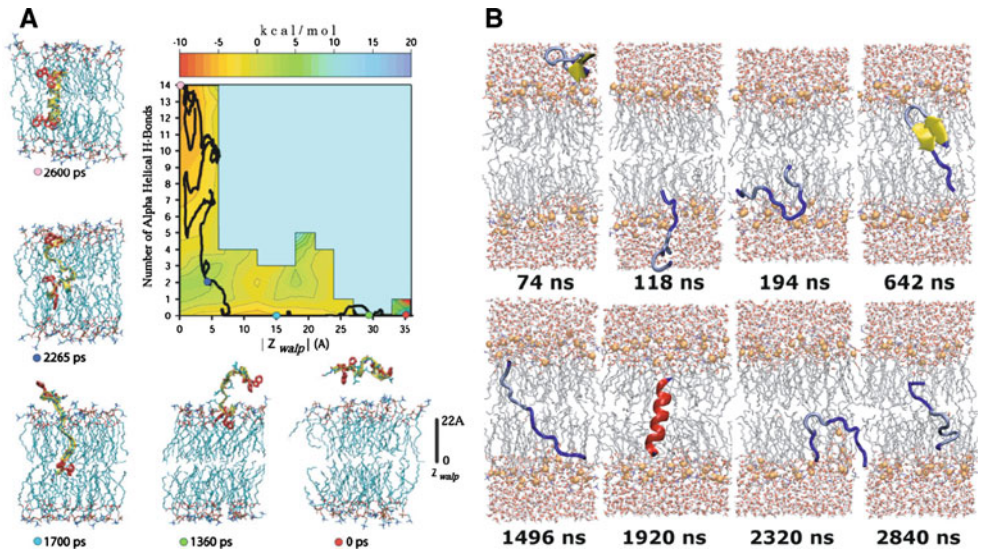


**Fig. 1** **a** Unfolded insertion as observed by a 3-ns atomic detail MD replica exchange simulation (Nymeyer et al. 2005). The progress along the free energy surface (**a**, *inset*) shows that insertion occurs before formation of hydrogen bonds and is associated with an energy drop. **b** Unfolded insertion and stable unfolded equilibrium configurations observed from a 3-μs direct partitioning MD simulation (Ulmschneider and Ulmschneider 2008a). Both simulations show erroneous unfolded insertion and stable unfolded conformers in the membrane. Adapted from Nymeyer et al. (2005) and Ulmschneider and Ulmschneider (2008a)

strongly suggests that unfolded conformers cannot exist in the bilayer core, and that interfacial helical folding will always precede peptide insertion into the bilayer (Jacobs and White 1989; Popot and Engelman 1990). The principle reason is the prohibitive cost of desolvating exposed (i.e., unformed) peptide bonds. Burial of an exposed peptide backbone is estimated to carry a penalty of ~0.5 kcal/mol per bond for transfer from the semiaqueous bilayer interface (Ladokhin and White 1999; Wimley et al. 1998; Wimley and White 1996) and ~4.0 kcal/mol per bond from bulk water (Ben-Tal et al. 1996, 1997; White 2006; White and Wimley 1999). As a consequence, lipid bilayers are powerful inducers of secondary structure formation, rapidly driving peptides into folded states. The observed erroneous behavior in the simulations was likely due to both incomplete sampling as well as a failure of the used force fields to accurately balance lipid–protein interactions.

In response, a new set of lipid parameters was developed using many microseconds of simulation time to accurately capture the key structural, dynamic, and thermodynamic properties of fluid lipid bilayers (Ulmschneider and Ulmschneider 2009b). Partitioning simulations with these new parameters in combination with OPLS-AA (Jorgensen et al. 1996) protein force field have confirmed the folded insertion pathway (Ulmschneider et al. 2010a).

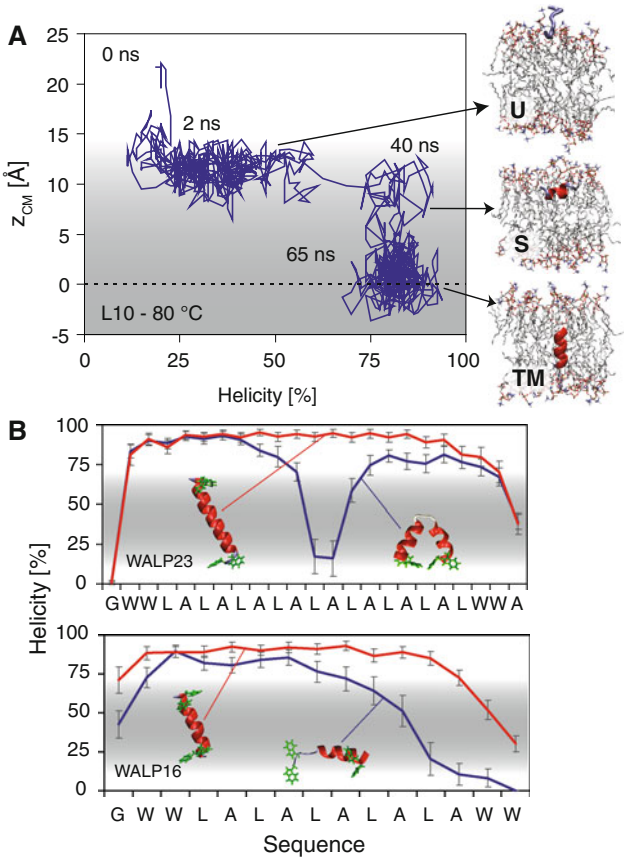


**Fig. 2** **a** Folded insertion pathway as observed for $L_{10}$ at 80°C. Shown is the insertion depth (center of mass z-position) as a function of peptide helicity. Adsorption to the interface from the unfolded initial state in water occurs in ~2 ns (U). The peptide then folds into a surface bound state (S) and subsequently inserts as a TM helix. **b** The S state is a horizontal surface bound helix for shorter peptides (WALP16), while longer sequences prefer a helix-turn-helix motif (WALP23). The TM state is always a uniform helix, independent of peptide length. Adapted from Ulmschneider et al. (2010a, b)

## Equilibrium Properties and Determining the Free Energy of Insertion

Partitioning simulations have now confirmed that the general pathways taken by membrane-inserting peptides consists of three steps: absorption, interfacial folding, and folded TM insertion, as illustrated for $Leu_{10}$ in Fig. 2a. The nonequilibrium phase (stages I and II) is usually completed in < 500 ns of simulation. Subsequently, strongly hydrophobic peptides (e.g., WALP) insert irreversibly (Ulmschneider et al. 2009), while the equilibrium for less hydrophobic peptides consists of flipping back and forth between folded interfacial and TM inserted orientations, with the secondary structure remaining α-helical (Ulmschneider et al. 2010a).

The equilibrium interfacial and TM states can be distinguished by their characteristic center of mass position along the membrane normal ($z_{CM}$) and helix tilt angle ($\theta$) (Fig. 3). The TM state is a deeply buried helix aligned along the membrane normal ($\theta < 20°$), independent of peptide length. In contrast, the interfacial state (S) is a horizontal surface bound helix for shorter peptides (e.g., WALP16) ($\theta \approx 90°$), while longer sequences can adopt helix-turn-helix motifs (WALP23) (Fig. 2b). Insertion depths vary depending on peptide hydrophobicity. By means of x-ray scattering, Hristova et al. (2001) found amphiphilic melittin peptides to reside near the glycerol carbonyl linker $z_{CM} \approx 17.5 \pm 0.2$ Å, while the highly hydrophobic peptides (WALP, polyL) studied by simulations so far bury more deeply at the edge of the acyl chains just below the glycerol/carbonyl groups ($z_{CM} \approx 12$ Å). A major advantage of the atomic models over mean-field or coarse-grained methods is that it is possible to observe in detail how peptides are accommodated into and perturb lipid bilayers, both in the interfacial and TM states (Fig. 4).

The partitioning equilibrium can be visualized by projecting the orientational free energy $\Delta G$ as a function of peptide tilt angle and center of mass position $z_{CM}$ along the membrane normal (Fig. 5). Generally membrane inserting peptides display characteristic S ($z_{CM} \approx \pm 15$ Å, $\theta \approx 90°$) and TM ($z_{CM} \approx 0$ Å, $\theta \approx 0°$) minima. Noninsertion peptides lack the TM state. Figure 5 shows the shift in partitioning equilibrium associated with lengthening polyleucine ($L_n$) peptides from $n = 5$ to 10 residues as

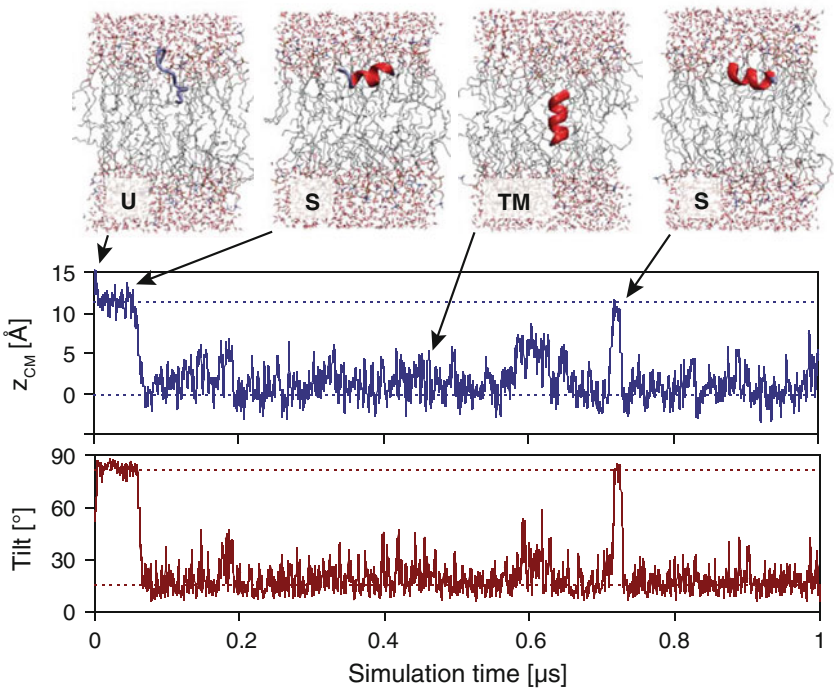


**Fig. 3** Equilibrium phase partitioning of the $L_{10}$ peptide at 80°C. Adsorption and folding from the unfolded initial state (U) occurs in ~5 ns. Subsequently, the peptide is found as either a surface (S) helix or a TM inserted helix, with a characteristic center of mass position along the membrane normal ($z_{CM}$) and helix tilt angle. Adapted from Ulmschneider et al. (2010b)

studied by Ulmschneider et al. (2010b). Overall, these free energy projections reveal a true and simple thermodynamic system: Only two states exist (S and TM), and they are both sufficiently populated to directly derive the free energy of insertion from

$$\Delta G_{S\to TM} = -RT \ln\left(\frac{p_{TM}}{p_S}\right) \quad (1)$$

Here $T$ is the temperature of the system, $R$ is the gas constant, and $p_{TM}$ the population of the TM inserted state. In the absence of other states, the free energy difference assumes the simple equation

$$\Delta G_{S\to TM} = RT \ln(1/p_{TM} - 1) \quad (2)$$

characteristic of a two-state Boltzmann system. Convergence is very important, so a high number of transitions between states is needed for $p_{TM}$ to be accurate. For peptides with a short hydrophobic stretch the interfacial state dominates and $\Delta G > 0$, while longer sequences mainly insert to form TM helices ($\Delta G < 0$). For very long peptides ($L_n$ with $n > 12$, WALP16, WALP23, etc.), the insertion into the TM state becomes irreversible as it is greatly favored over the interfacial helix, resulting in no equilibrium population of the S state ($p_{TM} = 100\%$). In this case, $\Delta G << 0$, and cannot reliably be calculated.

For $L_n$, the computational insertion propensities were found to correlate remarkably well with experimental apparent free energies for in vitro insertion of polyleucine segments via the Sec61 translocon (Jaud et al. 2009). Jaud et al. (2009) have previously shown that the experimental insertion propensity as a function of the number of leucine residues $n$ can be fitted perfectly to the sigmoidal function $p_n = [1 + \exp(-\beta\Delta G_n)]^{-1}$, where $\beta = 1/kT$. Figure 6 shows the experimental and computed insertion propensities together with the best-fit models ($R^2 > 0.99$). Both curves display two-state Boltzmann behavior, with a transition to TM inserted configurations for longer peptides. Figure 6b shows that $\Delta G_n$ increases perfectly linearly with $n$ in both simulations and experiment. Interestingly, the offset and slope vary slightly, reflecting a shift of the computed insertion probability curve toward shorter peptides by ~2.4 leucine residues, corresponding to a $\Delta\Delta G = \Delta G_{translocon} - \Delta G_{direct} = 1.91 \pm 0.01$ kcal/mol offset between the experimental and computational insertion free energies. At present the reason for this offset is not clear, but it is likely to reflect the difference between water-to-bilayer and translocon-to-bilayer peptide insertion.

## Partitioning Kinetics: Determination of the Insertion Barrier

A major advantage of the direct partitioning simulations is that the kinetics of the process can be calculated for the first time. However, because of the limited timescale of ~1–2 μs achievable in the MD simulations, this is difficult to estimate at ambient temperature. By increasing the simulation temperature, one can dramatically increase peptide insertion and expulsion rates. This is possible because hydrophobic peptides are remarkably thermostable

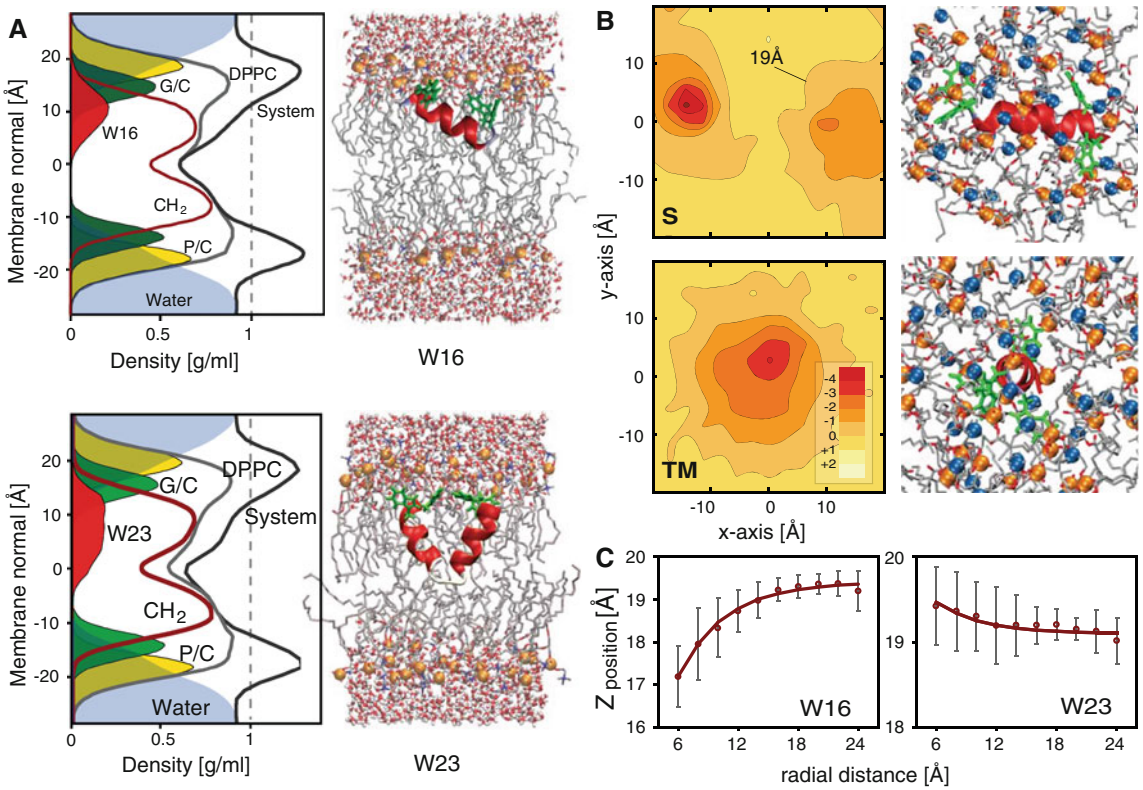


**Fig. 4** Bilayer deformation and accommodation of the peptides. **a** Density profiles of the bilayer shows that the S state of W16 and W23 is located just below the water interface. The terminal tryptophans are anchored in the interface, while the rest of the peptide is in contact mainly with the alkane tails ($CH_2$), with only a small overlap with the phosphocholine (PC) head groups and carbonylglycerol (CG) groups. **b** The equilibrium-phase time-averaged phosphate position from the bilayer center for the surface bound (S) and membrane spanning (TM) helix of W16 shows the peptide induced distortion to the bilayer, with the PC head groups covering the peptide in both configurations (the nitrogen atom of choline is represented as a blue sphere, and the phosphor atom of the phosphate is orange). Local thinning in the vicinity of the peptide is caused by the head groups bending over the helix in order to compensate for the bilayer expansion (~2%) caused by the peptide. Once inserted in a TM configuration, the head groups must cover the extra area of the W16 helix, leading to a circular decrease in bilayer width around the peptide, consistent with a negatively mismatched peptide. **c** Bilayer deformation in the vicinity of the TM helix. The time-averaged phosphate position along the membrane normal ($Z_{position}$) varies exponentially with radial distance from the peptide. For negatively mismatched W16, this results in a significant local decrease in bilayer width around the peptide, while W23 shows a slight positive mismatch. Adapted from Ulmschneider et al. (2010a)

in the presence of bilayers, generally remaining fully helical even at highly elevated temperatures of 90°C, irrespective of their insertion state (Ulmschneider et al. 2010a). The situation is radically different from globular proteins, which usually present an ensemble of conformations at equilibrium and are only marginally thermostable. Even modest heating causes radical changes to the ensemble as the peptide conformers denature. In contrast, peptide partitioning equilibria are not of structural ensembles but of fully folded helices in different membrane locations, at least for the monomeric systems considered here. As a result, no folding/unfolding events complicate the kinetic scheme, which corresponds to a simple two-state partitioning process of a rigid α-helix.

The partitioning kinetics for tryptophan flanked WALP16 and WALP23 peptides as well as an unflanked polyleucine ($L_8$) are summarized as Arrhenius plots in Fig. 7 (Ulmschneider et al. 2010a). In all cases, a fit of $k \sim \exp(-\beta \Delta H^{\ddagger})$ can be achieved (quality of fit $r^2 > 85\%$), indicating a first-order, single-barrier process. From this, both the activation enthalpy for insertion $\Delta H^{\ddagger}_{S \to TM}$ and expulsion $\Delta H^{\ddagger}_{TM \to S}$ can be determined (Table 1). For peptides without anchoring residues (e.g., aromatics or ionizable residues), the barriers for both insertion and expulsions are relatively weak: $L_8$ has an enthalpic barrier of $\Delta H^{\ddagger} \approx 5$–8 kcal/mol, with transition times of up to ~0.5 μs at 30°C (Ulmschneider et al. 2010a). This contrasts with the much higher $\Delta H^{\ddagger}_{S \to TM} = 23.3 \pm 5$ kcal/mol for WALP16 and $24.2 \pm 6$ kcal/mol for WALP23. Here, translocation of the anchoring Trp residues is the rate-limiting step, which can be seen from the apparent independence of the barrier on the length of the peptides. Extrapolated to room temperature (25°C), the insertion times are $\tau = 107 \pm 15$ ms for WALP16 and

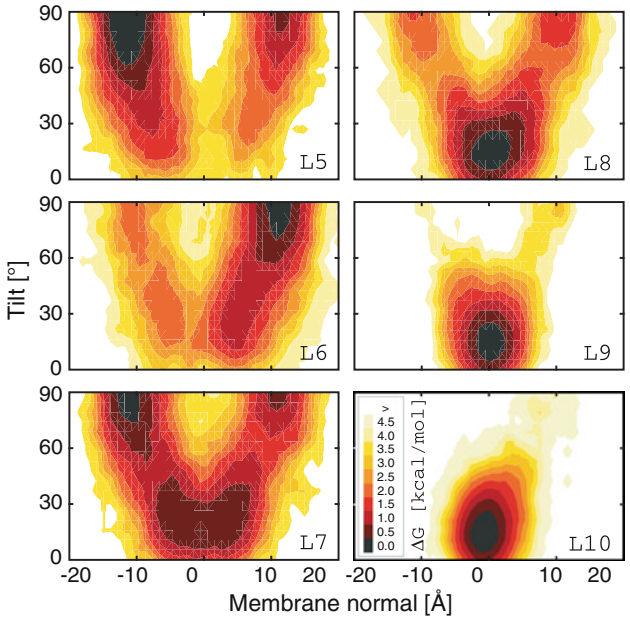


**Fig. 5** Free energy profile for $L_n$ peptides ($n = 5$–10), as a function of position along the membrane normal $z$ and tilt angle. Smaller peptides ($n \leq 7$) have interfacial minima ($z = \sim 12$ Å, $\alpha = \sim 90°$), while for longer sequences ($n \geq 8$) the TM inserted minima dominate ($z = \sim 0$ Å, $\alpha = \sim 10°$). The bilayer leaflets become visible by a division of the TM minimum for shorter peptides, whose TM helix hops between both leaflets. Adapted from Ulmschneider et al. (2010b)

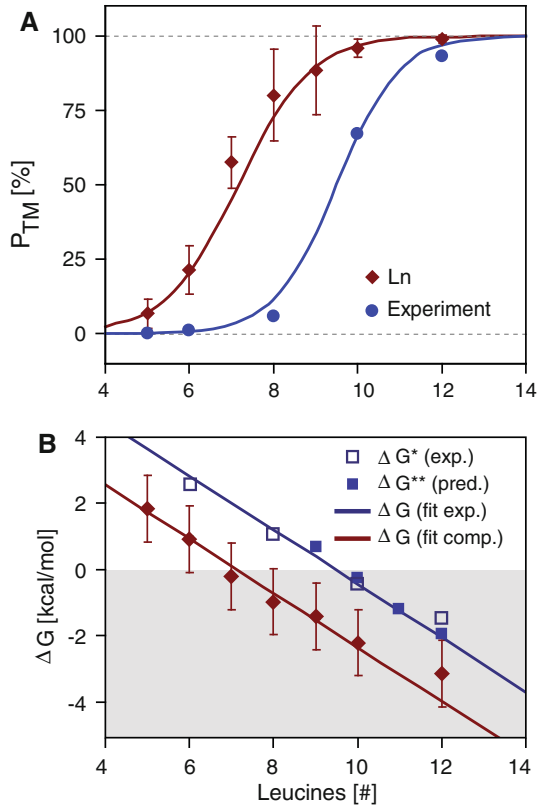


**Fig. 6** **a** Bilayer insertion efficiency as a function of peptide length $n$. The experimental values are for translocon-mediated insertion into dog pancreas rough microsomes of GGPG-(L)$_n$-GPGG constructs embedded into the leader peptidase carrier sequence, as determined by Jaud et al. (2009). The computed values are for spontaneous partitioning of ace-(L)$_n$-ame peptides into palmitoyloleoylphosphatidylcholine (POPC) lipid bilayers at 80°C. Both systems display perfect two-state Boltzmann behavior ($R^2 > 0.99$). **b** Free energy of insertion as a function of peptide length. The straight lines indicate the two-state Boltzmann fit, while the data points show the computed and experimental values for the individual peptides. *Measured $\Delta G$ (Hessa et al. 2007). **Predicted $\Delta G$ (http://dgpred.cbr.su.se/). There is a constant 1.91 ± 0.01 kcal/mol offset between the experimental and computational insertion free energies. Adapted from Ulmschneider et al. (2010b)

$\tau = 163 \pm 24$ ms for WALP23 (Table 1), which is beyond the timescales typically achievable in MD simulations. Even at elevated temperatures, expulsion rates cannot be obtained because this process is many orders of magnitude slower than insertion and is never observed in the simulations of these highly hydrophobic peptides. These results match well to time-resolved fluorescence experiments of a similar 25-residue hydrophobic peptide in dioleoylglycerophosphocholine (DOPC) vesicles (Meijberg and Booth 2002). There, Arrhenius-like kinetics were observed from 20–45°C, with an estimated activation energy of $\Delta H_{in}^{\ddagger} = 21 \pm 2$ kcal/mol, very similar to the 15–23 kcal/mol obtained here. However, insertion at 30°C ($\tau = 430$ s) was orders of magnitude slower than for WALP (~0.1 s). Future experiments and simulations will be required to clarify these issues.

## Partitioning Charged Side Chains

Aromatic and charged residues are more abundant at the end of TM segments, reflecting their preference for the head group region of the lipid bilayer (Ulmschneider et al. 2005; Ulmschneider and Sansom 2001; Yau et al. 1998). Besides anchoring membrane proteins in the bilayer, many charged residues also play significant functional roles. A striking example is the voltage-sensing component of virtually all voltage-gated ion channels, the S4 TM helix, containing four or more Arg residues (Aggarwal and MacKinnon 1996; Seoh et al. 1996; Swartz 2008). However, the burial of charge in the hydrophobic interior of a bilayer comes at a high price. The energetic penalty experienced by Arg residues close to bilayer center is estimated from continuum models to be in the range of 40 kcal/mol (Honig and Hubbell 1984). Even though the presence of a charged residue deep in the bilayer will undoubtedly be associated with unfavorable energetics to some degree, the static continuum models fail to account for the heterogeneity of the lipid bilayer. MD simulations, on the other hand, are better able to capture the structural dynamics associated with the perturbation of amphiphilic lipid molecules in a bilayer upon encountering a strong

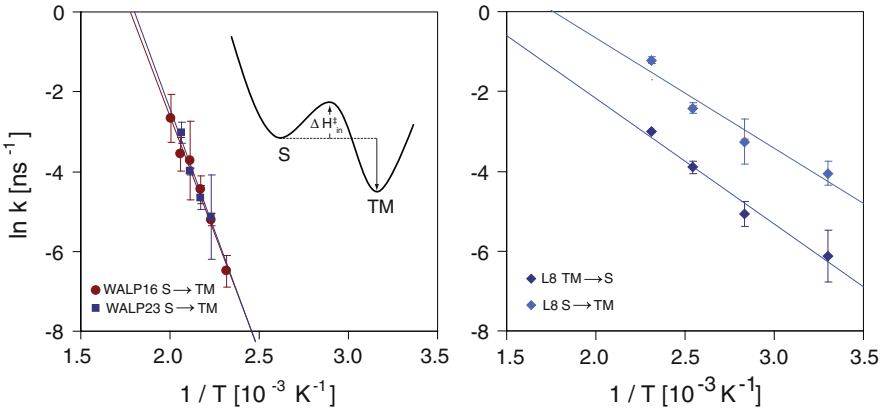


**Fig. 7** Partitioning kinetics at different temperatures. Arrhenius plots of the insertion and expulsion rates for WALP16, WALP23, and L8. The kinetics are approximately first order in all cases. The insertion of the WALP peptides is irreversible as the TM state is greatly favored. The insertion barrier of $\Delta H_{\text{in}}^{\ddagger} = 23$ kcal/mol is peptide length independent and caused by the terminal Trp residues. A much lower barrier of ~6 kcal/mol is found for the L8 peptide. Error bars are derived from block averages. Adapted from Ulmschneider et al. (2010a)

**Table 1** Partitioning kinetics of the L8 and WALP peptides

| | W16 | W23 | L8 |
|---|---|---|---|
| $\Delta H^{\ddagger}_{\text{SB}\to\text{TM}}$ [kcal/mol] | 23.3 ± 5 | 24.2 ± 6 | 5.5 ± 2 |
| $\Delta H^{\ddagger}_{\text{TM}\to\text{SB}}$ [kcal/mol] | – | – | 6.3 ± 2 |
| $\tau_{\text{SB}\to\text{TM}}$ ($T$ = 30°C) | 57 ± 9 ms | 85 ± 15 ms | 58 ± 17 ns |
| $\tau_{\text{TM}\to\text{SB}}$ ($T$ = 30°C) | – | – | 457 ± 162 ns |

The barrier heights $\Delta H^{\ddagger}$ are obtained from the slope of the Arrhenius plots. Transition times $\tau$ for L8 are from averaging at 30°C. $\tau$ for W16 and W23 is derived by extrapolating the Arrhenius plot to 30°C. No expulsion rates could be obtained for W16 and W23. Error estimates are from block averaging. Adapted from (Ulmschneider et al., 2010a)

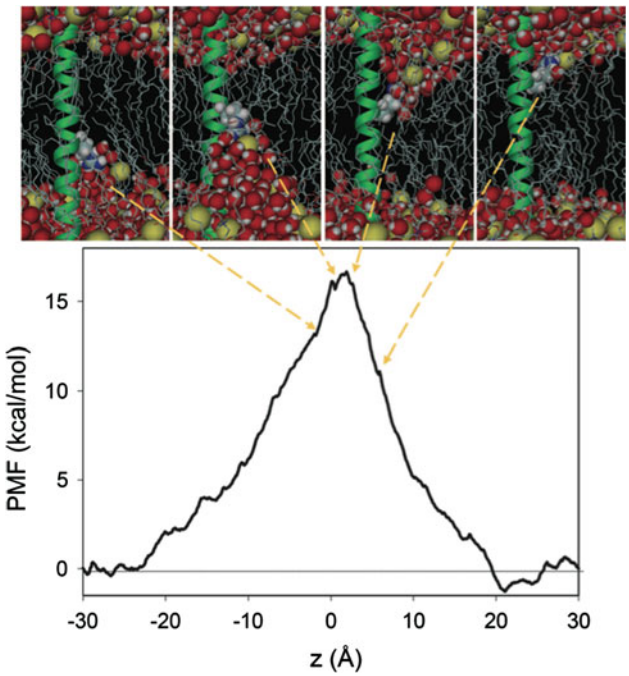


**Fig. 8** The PMF for an Arg residue on a poly-Leu TM helix (*bottom*), and MD snapshots depicting the deformation of the lipid bilayer upon insertion of the charged amino acid residue (*top*). Adapted from Dorairaj and Allen (2007), copyright (2007) National Academy of Sciences, USA

electric field imposed by a charged residue. A PMF, derived from MD simulations, is frequently used to demonstrate the variation of the solvation energetics for a certain amino acid residue along the normal to the bilayer (Fig. 8).

Typically, the PMF profile of a charged residue shows energy wells coinciding with the location of the polar head group region and then rises sharply near the hydrophobic center of the bilayer. The characteristics of a PMF profile are dependent to some degree on whether the calculation was based on a series of simulations of isolated amino acid side chain analogues at different positions along the normal of the bilayer or, rather, on a target residue moved alongside a TM helix (Allen 2007; Li et al. 2008b). Although using a side chain analogue will typically require much shorter equilibration times, all influence from a TM helix is lost, such as amino acid side chains interacting with the protein backbone or being allowed to snorkel into the head group region of the bilayer (Johansson and Lindahl 2006, 2008, 2009a; MacCallum et al. 2008). As a result, the charged amino acid analogue experiences an increased flexibility in the absence of a helix and its favorable interactions to the polar head group region are thereby overestimated (Allen 2007; Li et al. 2008b). Moreover, Arg analogues have been shown to have greater hydration numbers, by two to three water molecules compared to Arg side chains, in bulk water. This was expected to lower the free energy of solvation in the bulk water reference state,

leading to an exaggerated barrier of insertion into the bilayer (Li et al. 2008a). Regardless of the method used, MD simulations illustrate a common theme of all charged amino acids, they interact favorably with water molecules and polar head groups at the edge of the bilayer (Dorairaj and Allen 2007; Johansson and Lindahl 2006, 2008, 2009a; Li et al. 2008a; MacCallum et al. 2007, 2008). The basic Lys and Arg residues are able to form H-bonds to the phosphate groups of the lipid head groups as well as to the carbonyl groups, which are located further into the bilayer. Acidic residues, on the other hand, are only able to H-bond to the more distal choline groups and will thus show less pronounced energy wells at the edges of the bilayer compared to basic residues (Johansson and Lindahl 2008). Interestingly, the PMF profiles of basic and acidic residues has also been shown to be highly dependent on the charge of the lipid molecules (Johansson and Lindahl 2009a). Although the maximum insertion barrier was comparable for Arg insertion between the investigated lipids, the shape of the profile varied significantly with lipid charge. The zwitterionic, neutral DOPC and the negatively charged palmitoyloleoylphosphatidylglycerol (POPG) bilayers both showed advantageous energetics in the head group region, while the positively charged dioleoyltrimethylammonium-propane (DOTAP) bilayer did not. The unfavorable energetics in the DOTAP bilayer was attributed the lack of lipid phosphates in this bilayer, which would provide H-bonding possibilities for the charged Arg residue.

As a charged residue moves beyond the favorable interactions in the lipid head group region into the hydrophobic core, the bilayer will demonstrate its amazing adaptive abilities. The behavior of a bilayer upon encountering a heavily charged peptide, based on the S4 sequence, was illustrated by Freites et al. (2005) (Fig. 9). The effective bilayer thickness was reduced in the vicinity of the TM helix as lipid phosphates and water molecules were pulled into they bilayer to provide a stabilizing H-bonding network around the snorkeling Arg residues. This type of local bilayer deformation creates two hydrophilic compartments, at each end of the helix, that help solvate charged residues in the bilayer interior. The reduction of the hydrophobic interior was accompanied by the formation of a highly focused electric field in the vicinity of the TM helix. Vorobyov et al. (2010) also observe substantial membrane deformations, caused by the introduction of a charged Arg side chain analogue, causing substantial disruption of the dipole potential. The Arg analogue was shown to always assume a position at the interface between the low-potential region of the water-filled deformation and the high-potential region of the hydrophobic core. In fact, the charged Arg residue remained hydrated and never crossed the interface, it rather reshaped it while moving toward the bilayer center and so never faced the full potential. The work performed against the electric field is what determines the shape of the PMF profile.

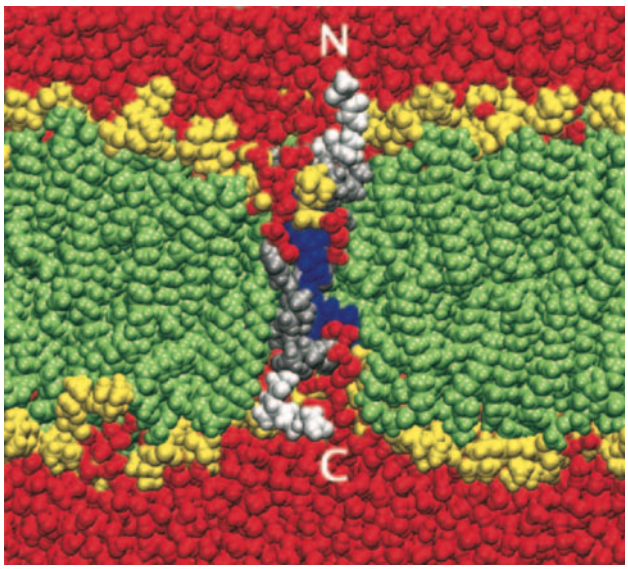


**Fig. 9** Simulation snapshot of a model S4 voltage-sensor peptide in a palmitoyloleoylphosphatidylcholine (POPC) bilayer, showing bilayer distortion around the peptide as the Arg residues become solvated by lipid phosphates and water molecules. Adapted from Freites et al. (2005), copyright (2005) National Academy of Sciences, USA

For a bilayer deformation to form, its energetic cost must be counterbalanced by the free energy of solvating the side chain. In particular, solvation of the ionized forms of Asp, Glu, Lys, and Arg are favorable enough for maintaining large membrane deformations (MacCallum et al. 2008). In contrast, no major bilayer perturbations are observed upon solvation of their neutral counterparts and the free energy of insertion for these residues seem to be governed solely by simple dehydration (Allen 2007). A prediction of acidic and basic side chain $pK_a$ values inside the bilayer would therefore indicate the maximum depth at which the solvation of a charged residue might be upheld by membrane deformations. MacCallum et al. (2008) report the $pK_a$ values of Asp and Glu to move above 7.0 at the bilayer interface, while the basic amino acids stay charged at much greater bilayer depths. The $pK_a$ for Lys does not fall below 7.0 until 4 Å from the center of the bilayer. The high $pK_a$ of 12.0–13.7 (Angyal and Warburton 1951; Hall and Sprinkle 1932; Nozaki et al. 1967) of Arg in aqueous solution suggests an even greater penetration ability of its charge. Indeed, several studies show that the $pK_a$ of Arg do not fall below 7.0 until the center of the bilayer, where enormous deformations of the bilayer help stabilizing its charge (Li et al. 2008a, 2008b; MacCallum et al. 2007, 2008). To further explore the influence the choice of methodology might have on this result, Allen and

coworkers (Allen 2007; Li et al. 2008a, 2008b) contrasted a free Arg side chain analogue against a helix-attached Arg side chain simulation and found that energy wells and peak regions of the corresponding PMF profiles differed significantly (Fig. 10a), for reasons discussed above, and that bilayer deformations were absent for neutral species and present only when the residues were charged. In fact, the calculated $pK_a$ shift for the Arg side chain remained unaffected until reaching the 10 Å central portion of the bilayer, where it dropped by −4.5 units, resulting in a $pK_a$ of 7.5–9.2 still indicative of a charged Arg side chain (Fig. 10b). The pKa shift for the analogue, however, is exaggerated and would result in a deprotonated Arg in the bilayer center, denoting the importance of the TM segment upon simulating partition dynamics. The unique

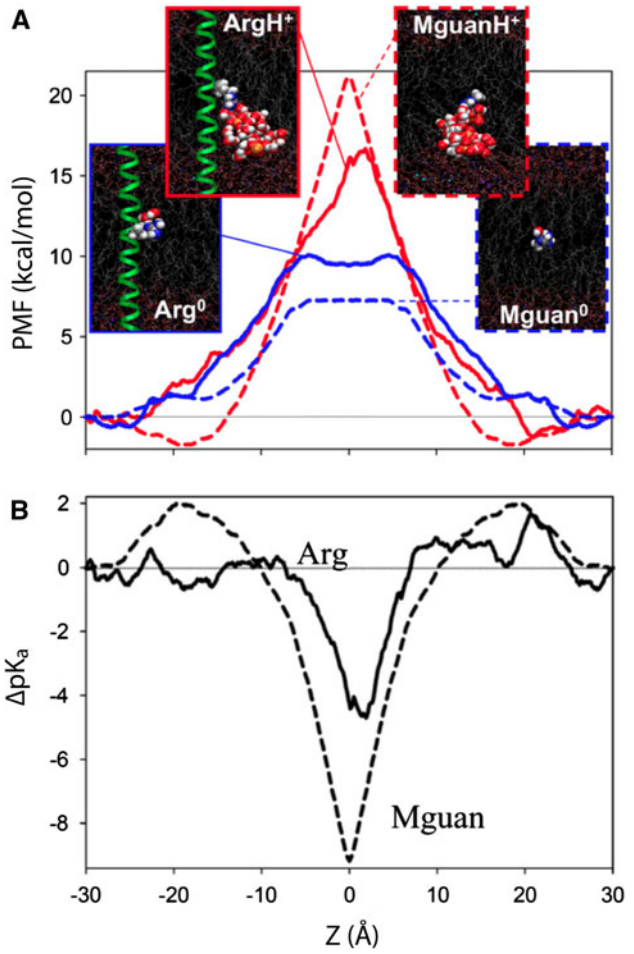


**Fig. 10** **a** PMFs for Arg side chains (Arg), both protonated ($ArgH^+$) and deprotonated ($Arg^0$). The corresponding Arg side chain analogues are shown as *dashed lines*. *Insets* show snapshots from the MD simulations at the center of the bilayer ($z = 0$ Å). Adapted from Li et al. (2008b). **b** The $pK_a$ shift profile for an Arg side chain (*solid line*) and an Arg side chain analogue (Mguan, *dashed line*). Adapted from Li et al. (2008a)

penetration depth of charged Arg residues might explain the evolutionary preference of Arg over Lys in the S4 sensor of the voltage-gated K + channel (Jiang et al. 2003), since positive gating charges are absolutely required in order for the channel to respond to changes in the membrane potential (Aggarwal and MacKinnon 1996; Seoh et al. 1996; Swartz 2008).

The image of a charged Arg residue residing deep within the hydrophobic core of the bilayer, coordinated by a network of lipid phosphates and water molecules by means of bilayer deformations, is illustrative in light of a groundbreaking experiment, wherein a model helix based on the sequence of the S4 sensor was shown to become efficiently inserted into the endoplasmic reticulum (ER) membrane (Hessa et al. 2005b). Hessa et al. further utilized their translocon-mediated insertion system to derive an in vivo biological hydrophobicity scale (Hessa et al. 2005a), which show a surprisingly low energy penalty (∼2.5 kcal/mol) for the introduction of an Arg residue in the middle of a hydrophobic TM helix. While showing a close correspondence to the Wimley–White n-octanol scale (White and Wimley 1999; Wimley et al. 1996), scales derived from MD simulations report values typically a factor of 3–4 times higher (Dorairaj and Allen 2007; Johansson and Lindahl 2009a; MacCallum et al. 2008). This discrepancy has been attributed to the complexity of the biological system and, in particular, the absence of a well characterized inserted state (Allen 2007; Hessa et al. 2005a; Johansson and Lindahl 2009b; MacCallum et al. 2007; Ulmschneider et al. 2010b; Von Heijne 2007; White 2007). However, as pointed out by von Heijne (2007) and White (2007), one should bear in mind that the biological scale is not measuring a direct bulk-to-bilayer partitioning per-se but rather translocon-mediated bilayer insertions. Furthermore, the high success rate at which the biological scale predicts membrane protein topologies (Bernsel et al. 2008), significantly strengthens its validity. In an attempt to model the insertion of an Arg residue into a biological membrane as realistically as possible, Johansson et al. (2009b) performed MD simulations where the bilayer included extra TM helices as well as a translocon. At a certain mass fraction of added TM helices, the solvation free energy of Arg was found to reach the experimental value of 2.5 kcal/mol and the presence of a translocon lowered the cost of inserting an Arg reside to 3–5 kcal/mol right next to the lateral gate. These results were ascribed to the presence of extra helices in the bilayer, making it possible for the membrane to retain more hydration water, not only in the interfacial region, but also closer to the hydrophobic core. This connects well to the conclusion by White (2007) that the insertion of charge-bearing TM helices in the studies by Hessa et al. (2005a, b) can be explained by a combination of charged residue snorkeling and local lipid

rearrangements in the immediate vicinity of the charge-bearing helices.

## Conclusions and Perspective

The results reviewed here demonstrate that peptide–membrane partitioning phenomena can now be studied in their entirety by conventional atomic detail MD simulations, without the need for millisecond sampling times as previously thought. Virtually all membrane active peptides can in principle be considered, opening up the possibility to quickly gather kinetic data (e.g., room-temperature insertion rates from extrapolation of high-temperature behavior) and thermodynamic data (insertion propensities) on many of these systems using modest computational effort. Where barriers are high as a result of the presence of charged residues, PMF calculations offer a convenient alternative, albeit at the loss of kinetic information.

Full peptide water-to-bilayer transfer properties allow the construction of a complete insertion scale for arbitrary sequences, answering how strongly membrane proteins are embedded into lipid bilayers. Because these properties are critical to the structural stability of membrane proteins and consequently their function, their accurate theoretical description and precise quantification are of the utmost importance. It is unfortunately difficult to extract similar information from experiments because the design of monomerically partitioning peptides has remained an unsolved challenge (Ladokhin and White 2004; Wimley and White 2000).

However, recent in vitro experiments that used the microsomal Sec61 translocon machinery have allowed the construction of an insertion scale for arbitrary sequences (Hessa et al. 2005a, 2007). Although this cannot at present be directly compared to the monomeric peptides simulations, the agreement is nevertheless very close. It is desirable that in the near future a quantitative match between experimental and simulated insertion free energies can be achieved. As MD enters the millisecond timescale over the coming decade, simulations of membrane active peptides and membrane proteins will provide a powerful new tool to complement experiments.

**Acknowledgments** This research was supported by an EU Marie Curie International Fellowship to MBU, a BIOMS fellowship to JPU, the U.S. National Institutes of Health grants RO1 GM74737 from NIGMS and Program Project Grant PO1 GM86685 from the NIGMS and NINDS, both to SHW. We are grateful for allocation of computer time on the NSF-supported TeraGrid resources provided by the Texas Advanced Computing Center.



## References

Aggarwal SK, MacKinnon R (1996) Contribution of the S4 segment to gating charge in the Shaker $K^+$ channel. Neuron 16:1169–1177

Allen TW (2007) Modeling charged protein side chains in lipid membranes. J Gen Physiol 130:237–240

Angyal SJ, Warburton WK (1951) The basic strengths of methylated guanidines. J Chem Soc 2492–2494

Babakhani A, Gorfe AA, Kim JE, McCammon JA (2008) Thermodynamics of peptide insertion and aggregation in a lipid bilayer. J Phys Chem B 112:10528–10534

Ben-Tal N, Ben-Shaul A, Nicholls A, Honig B (1996) Free-energy determinants of alpha-helix insertion into lipid bilayers. Biophys J 70:1803–1812

Ben-Tal N, Sitkoff D, Topol IA, Yang AS, Burt SK, Honig B (1997) Free energy of amide hydrogen bond formation in vacuum, in water, and in liquid alkane solution. The J Phys Chem B 101:450–457

Bernsel A, Viklund H, Falk J, Lindahl E, von Heijne G, Elofsson A (2008) Prediction of membrane-protein topology from first principles. Proc Natl Acad Sci USA 105:7177–7181

Dorairaj S, Allen TW (2007) On the thermodynamic stability of a charged arginine side chain in a transmembrane helix. Proc Natl Acad Sci USA 104:4943–4948

Freddolino PL, Liu F, Gruebele M, Schulten K (2008) Ten-microsecond molecular dynamics simulation of a fast-folding WW domain. Biophys J 94:L75–L77

Freites JA, Tobias DJ, von Heijne G, White SH (2005) Interface connections of a transmembrane voltage sensor. Proc Natl Acad Sci USA 102:15059–15064

Gurtovenko AA, Anwar J, Vattulainen I (2010) Defect-mediated trafficking across cell membranes: insights from in silico modeling. Chem Rev 13:6077–6103

Hall NF, Sprinkle MR (1932) Relations between the structure and strength of certain organic bases in aqueous solution. J Am Chem Soc 54:3469–3485

Hessa T, Kim H, Bihlmaier K, Lundin C, Boekel J, Andersson H, Nilsson I, White SH, von Heijne G (2005a) Recognition of transmembrane helices by the endoplasmic reticulum translocon. Nature 433:377–381

Hessa T, White SH, von Heijne G (2005b) Membrane insertion of a potassium-channel voltage sensor. Science 307:1427

Hessa T, Meindl-Beinker NM, Bernsel A, Kim H, Sato Y, Lerch-Bader M, Nilsson I, White SH, von Heijne G (2007) Molecular code for transmembrane-helix recognition by the Sec61 translocon. Nature 450:1026–1030

Honig BH, Hubbell WL (1984) Stability of "salt bridges" in membrane proteins. Proc Natl Acad Sci USA 81:5412–5416

Hristova K, Dempsey CE, White SH (2001) Structure, location, and lipid perturbations of melittin at the membrane interface. Biophys J 80:801–811

Im W, Brooks CL (2005) Interfacial folding and membrane insertion of designed peptides studied by molecular dynamics simulations. Proc Natl Acad Sci USA 102:6771–6776

Jacobs RE, White SH (1989) The nature of the hydrophobic binding of small peptides at the bilayer interface: implications for the insertion of transbilayer helices. Biochemistry 28: 3421–3437

Jaud S, Fernandez-Vidal M, Nilsson I, Meindl-Beinker NM, Hubner NC, Tobias DJ, von Heijne G, White SH (2009) Insertion of

short transmembrane helices by the Sec61 translocon. Proc Natl Acad Sci USA 106:11588–11593
Jiang Y, Lee A, Chen J, Ruta V, Cadene M, Chait BT, MacKinnon R (2003) X-ray structure of a voltage-dependent $K^+$ channel. Nature 423:33–41
Johansson AC, Lindahl E (2006) Amino-acid solvation structure in transmembrane helices from molecular dynamics simulations. Biophys J 91:4450–4463
Johansson AC, Lindahl E (2008) Position-resolved free energy of solvation for amino acids in lipid membranes from molecular dynamics simulations. Proteins 70:1332–1344
Johansson AC, Lindahl E (2009a) The role of lipid composition for insertion and stabilization of amino acids in membranes. J Chem Phys 130:185101–185108
Johansson ACV, Lindahl E (2009b) Protein contents in biological membranes can explain abnorma; solvation of charged and polar residues. Proc Natl Acad Sci USA 106:15684–15689
Jorgensen WL, Maxwell DS, Tirado-Rives J (1996) Development and testing of the OPLS all-atom force field on conformational energetics and properties of organic liquids. J Am Chem Soc 118:11225–11236
Killian JA (2003) Synthetic peptides as models for intrinsic membrane proteins. FEBS Lett 555:134–138
Ladokhin AS, White SH (1999) Folding of amphipathic alpha-helices on membranes: energetics of helix formation by melittin. J Mol Biol 285:1363–1369
Ladokhin AS, White SH (2004) Interfacial folding and membrane insertion of a designed helical peptide. Biochemistry 43:5782–5791
Li L, Vorobyov I, Allen TW (2008a) Potential of mean force and pKa profile calculation for a lipid membrane–exposed arginine side chain. J Phys Chem B 112:9574–9587
Li L, Vorobyov I, MacKerell AD Jr, Allen TJ (2008b) Is arginine charged in a membrane? Biophys J 94:L11–L13
Lindahl E, Sansom MSP (2008) Membrane proteins: molecular dynamics simulations. Curr Opin Struct Biol 18:425–431
MacCallum JL, Bennett WFD, Tieleman DP (2007) Partitioning of amino acid side chains into lipid bilayers: results from computer simulations and comparison to experiment. J Gen Physiol 129:371–377
MacCallum JL, Bennett WF, Tieleman DP (2008) Distribution of amino acids in a lipid bilayer from computer simulations. Biophys J 94:3393–3404
Meijberg W, Booth PJ (2002) The activation energy for insertion of transmembrane alpha-helices is dependent on membrane composition. J Mol Biol 319:839–853
Nozaki Y, Tanford C, Hirs CHW (1967) Examination of titration behavior In Methods in Enzymology. Academic Press, pp 715–734
Nymeyer H, Woolf TB, Garcia AE (2005) Folding is not required for bilayer insertion: replica exchange simulations of an alpha-helical peptide with an explicit lipid bilayer. Proteins 59:783–790
Popot JL, Engelman DM (1990) Membrane-protein folding and oligomerization—the 2-stage model. Biochemistry 29:4031–4037
Seoh SA, Sigg D, Papazian DM, Bezanilla F (1996) Voltage-sensing residues in the S2 and S4 segments of the Shaker $K^+$ channel. Neuron 16:1159–1167
Swartz KJ (2008) Sensing voltage across lipid membranes. Nature 456:891–897
Ulmschneider MB, Sansom MSP (2001) Amino acid distributions in integral membrane protein structures. Biochim Biophys Acta Biomembr 1512:1–14
Ulmschneider JP, Ulmschneider MB (2007) Folding simulations of the trans-membrane helix of virus protein U in an implicit membrane model. J Chem Theory Comput 3:2335–2346
Ulmschneider MB, Ulmschneider JP (2008a) Folding peptides into lipid bilayer membranes. J Chem Theory Comput 4:1807–1809
Ulmschneider MB, Ulmschneider JP (2008b) Membrane adsorption, folding, insertion and translocation of synthetic trans-membrane peptides. Mol Membr Biol 25:245–257
Ulmschneider JP, Ulmschneider MB (2009a) Sampling efficiency in explicit and implicit membrane environments studied by peptide folding simulations. Proteins 75:586–597
Ulmschneider JP, Ulmschneider MB (2009b) United atom lipid parameters for combination with the optimized potentials for liquid simulations all-atom force field. J Chem Theory Comput 5:1803–1813
Ulmschneider MB, Ulmschneider JP (2010) Implicit membrane models for peptide folding and insertion studies. In: Sansom MSP, Biggin PC (eds) Molecular simulations and biomembranes: from biophysics to function. Royal Society of Chemistry
Ulmschneider MB, Sansom MS, Di Nola A (2005) Properties of integral membrane protein structures: derivation of an implicit membrane potential. Proteins 59:252–265
Ulmschneider JP, Doux JPF, Killian JA, Smith JC, Ulmschneider MB (2009) Peptide partitioning and folding into lipid bilayers. J Chem Theory Comput 5:2202–2205
Ulmschneider MB, Doux JPF, Killian JA, Smith J, Ulmschneider JP (2010a) Mechanism and kinetics of peptide partitioning into membranes. J Am Chem Soc 132:3452–3460
Ulmschneider MB, Smith JC, Ulmschneider JP (2010b) Peptide partitioning properties from direct insertion studies. Biophys J 98:L60–L62
Von Heijne G (2007) Formation of transmembrane helices in vivo—is hydrophobicity all that matters? J Gen Physiol 129:353–356
Vorobyov I, Bekker B, Allen TW (2010) Electrostatics of deformable lipid membranes. Biophys J 98:2904–2913
White SH (2006) How hydrogen bonds shape membrane protein structure. Adv Protein Chem 72:157–172
White SH (2007) Membrane protein insertion: the biology–physics nexus. J Gen Physiol 129:363–369
White SH, Wimley WC (1999) Membrane protein folding and stability: physical principles. Annu Rev Biophys Biomol Struct 28:319–365
Wimley WC, Creamer TP, White SH (1996) Solvation energies of amino acid side chains and backbone in a family of host–guest pentapeptides. Biochemistry 35:5109–5124
Wimley WC, Hristova K, Ladokhin AS, Silvestro L, Axelsen PH, White SH (1998) Folding of beta-sheet membrane proteins: a hydrophobic hexapeptide model. J Mol Biol 277:1091–1110
Wimley WC, White SH (1996) Experimentally determined hydrophobicity scale for proteins at membrane interfaces. Nat Struct Biol 3:842–848
Wimley WC, White SH (2000) Designing transmembrane alpha-helices that insert spontaneously. Biochemistry 39:4432–4442
Yau WM, Wimley WC, Gawrisch K, White SH (1998) The preference of tryptophan for membrane interfaces. Biochemistry 37:14713–14718